Ultrasonic underside inspection for fatigue cracks in the deck plate of a steel orthotropic bridge deck

M.C.M. Bakker[1] [1] and F.B.P. de Jong[2] [2,3]

[1] Delft University of Technology, Aerospace Materials Laboratory,
Department of Aerospace Engineering, Kluyverweg 1, 2629 HS Delft, The Netherlands.
[1] E-mail: m.c.m.bakker@lr.tudelft.nl

[2] Delft University of Technology, Section of Steel and Timber structures,
Department of Civil Engineering, Stevinweg 1, 2628 CN Delft, The Netherlands.

[3] Ministry of Transport, Public Works and Water Management Civil Engineering
Division, Section Steel and Mechanical Engineering,
P.O. Box 59, 2700 AB Zoetermeer, The Netherlands.
[2] E-mail: f.b.p.dejong@bwd.rws.minvenw.nl

Due to an unexpected increase of heavy traffic large fatigue cracks appeared through the deck plate of orthotropic steel bridge decks in the Netherlands. Visual inspection revealed that this particular type of crack initiates where a weld joins the deck plate, a rib and a girder. These critical points are commonly inspected from the roadside, which necessitates that the road is closed down for all traffic and that the wear layer is first removed. To overcome these costly drawbacks a new method is proposed that enables ultrasonic inspection of the deck plate from the underside of the bridge deck. The method requires a combination of two special measurement techniques, which are optimised for the bridge problem at hand. To detect the maximum crack depth an angled pitch-catch technique is employed. The crack length can be detected along the rib weld by employing the simpler pulse-echo technique. The crack depth and crack length are determined from the respective ultrasonic data sets by a calibration, which relates the number of detected waves to the actual crack size. The calibration is determined by ultrasonically monitoring the various crack stages during a fatigue test that is conducted on a bridge deck specimen. The original, uncracked state and the final state where the cracks can be visibly detected in the deck plate determine the extremes. The tests show that a reasonable accurate detection of crack size is quite possible, while the visual inspections prove to be useless until the crack has already grown completely through the deck plate. The new method provides a crack depth and crack length estimate with an accuracy of ±15%.

Key words: ultrasonic inspection, fatigue crack, orthotropic bridge deck, steel

1 Introduction

During the last few decades the amount of road traffic in the Netherlands has increased considerably. This necessitates more inspection of bridges and leads to more repairs. The fatigue aspect received extra attention when in 1997 large cracks unexpectedly appeared right through the steel deck plate of some orthotropic bridge decks [1]. Although the cracks do not compromise the structural safety of the bridge itself, they could pose a danger to the traffic.

Visual (destructive) inspection revealed that this particular crack initiates where the deck plate, a trapezoidal rib and a girder are welded together, see Fig. 1. Therefore, this crack grows upwards from the bottom of the deck plate where it starts hidden from view inside the rib casing. This crack becomes visible only when it breaks through the upper surface of the deck plate.

With most commercial inspection methods these critical areas can be inspected only from the roadside. For this purpose the eddy-current technique or a visual technique like dye penetrant [2] may be employed. These well known techniques are useable only when the crack is (practically) through the deck plate. For early crack detection and more accurate depth sizing time-of-flight diffraction technique (TOFD) [3] could be applied. However, for all three of these techniques the road has to be closed for all traffic and the wear layer has to be removed first.

To overcome these major drawbacks inspection should take place at the underside of the bridge deck. At first hand, the acoustic emission technique [4,5] seems to be a viable option. However, it requires heavy traffic to impose the dynamic loading that activates crack sound emission. Moreover, since AE sensors are highly sensitive and omnidirectional, the interpretation of the data may prove quite difficult due to other mechanical noise that may be picked up from all sides of the bridge deck.

In this paper, the inspection problem is tackled by first investigating a suitable method of ultrasonic [6] data acquisition. In an ultrasonic inspection the possible crack locations are irradiated with high-frequency waves. The waves that are reflected and scattered by a crack are detected and provide information on its size and position. The generation and detection of the waves is performed with special wave transducers [6].

A robust calibration method is applied to determine the crack size from the ultrasonic data. The method of calibration will allow the suppression of the influence of the unavoidable wave scattering due to the normal weld geometry. This unpredictable type of wave scattering always shows up in the data and could otherwise complicate their interpretation. The calibration is obtained by performing a sequence of fatigue tests on a bridge deck specimen until cracks are visibly detectable at the roadside of the deck plate. In each stage of cracking, ultrasonic measurements are taken.

A future development will be the application of advanced crack characterization techniques, such as the synthetic aperture focusing technique (SAFT) [7,8], which may retrieve more accurate infor-

mation concerning crack size and crack angle. These advanced techniques require accurate and reproducible data, to which end we have set three design criterions for the present data acquisition method.

First, measurements can be taken only on the flat steel surface in between the ribs at the underside of the bridge deck. Second, the data acquisition method must be optimised to ensure a good probability of detection (POD) [9], which in turn ensures that a crack will be detected whatever its possible size or angle.
Third, the acquisition method should be suitable for future implementation in an automated inspection tool [10] to enable large-scale application under practical conditions.

The third criterion has been met by employing data scanning along a straight line (line scans) [6], which requires only a translation movement of the receiving wave transducer. Reproducible positioning of the automated tool on the underside of the bridge deck will be facilitated by the convenient positioning references used for the transducers in this paper.

Section 1 describes the bridge deck specimen and the fatigue set-up, and Section 2 deals with the optimised measurement methods. In Section 3 we discuss the ultrasonic crack indicators and present the experimental results. In Section 4 we give our conclusions.

2 Bridge deck specimen and fatigue set-up

For an investigating of the ultrasonic inspection method the type of loading and other fatigue set-up details are of secondary interest, because they have no bearing on the performance of the inspection method.
The relevant part of the fatigue set-up is the specimen itself, its geometrical construction, the material it is made of and the type and location of the cracks that are to be found and characterized.

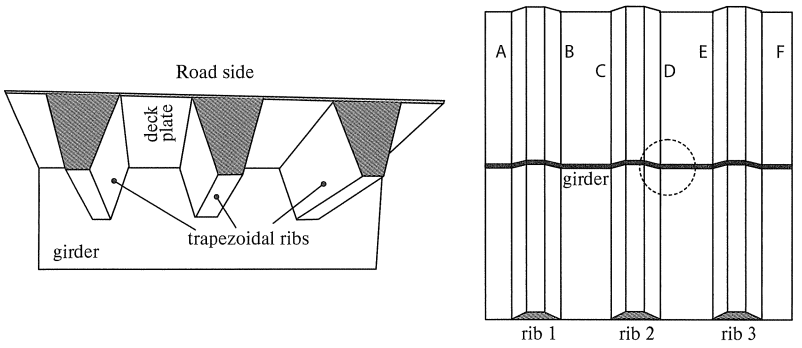

Figure 1: Left: Construction of a steel orthotropic bridge deck. Right: Bottom view on the bridge deck specimen and its rib welds.

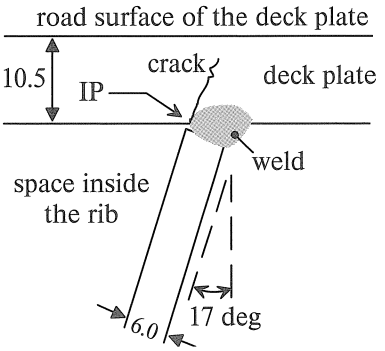

Figure 2: Vertical cross section of the crack initiation zone.

Nevertheless, to place the results in the proper context of the performed mechanical tests we describe not only the test specimen but also briefly the fatigue set-up.

The left panel in Fig. 1 shows the structural elements of the 2x2 meter bridge deck specimen. The specimen is fabricated according to the required Dutch specifications, but without the usual coatings or wear layer. The specimen has three steel trapezoidal ribs that are first welded onto the bottom of the steel deck plate. Subsequently the steel girder is welded over the ribs and onto the deck plate. The thickness of the deck plate is 10.5 mm, of the rib plating 6 mm, and of the girder 12 mm. At the deck plate a rib is 320 mm wide and its walls make a slope of 17 deg, as shown in detail in Fig. 2. The spacing between two different ribs is also 320 mm. The right panel in Fig. 1 shows a bottom view on the bridge deck, where the deck plate surface in between the ribs is available for ultrasonic data acquisition. For later reference the three ribs are numbered and the six rib welds are denoted from 'A' to 'F'.

Each passing wheel of a car or truck will cause fatigue of the bridge deck. This fatigue loading is simulated by cyclic loading at 1 Hz on the roadside of the bridge deck, applied in the middle of a rib and symmetrically over the girder. The loading is imposed first simultaneously at the outer ribs (ribs 1 and 3), and subsequently only at the middle rib (rib 2). The top-top amplitude of the cyclic force is 64 kN per loading area of 270 mm in the length direction and 320 mm in the width direction of the deck, which area simulates the tire impression of a big truck. The girder is fixed below to the steel loading frame and the deck is horizontally restrained at two places at each side to mimic the behaviour of a part of a much bigger bridge deck. The deck and the loading, as applied at the outer ribs, are shown in Fig. 3.

During the fatigue testing the strain in the deck plate at the girder-rib intersections was monitored on the roadside with strain gauges. The strain gauges have been used for the purpose of mechanical characterization of the deck, which results will be described in detail in a later publication. The only interest for the ultrasonic inspection is that the measured strain served as an indicator to sus-

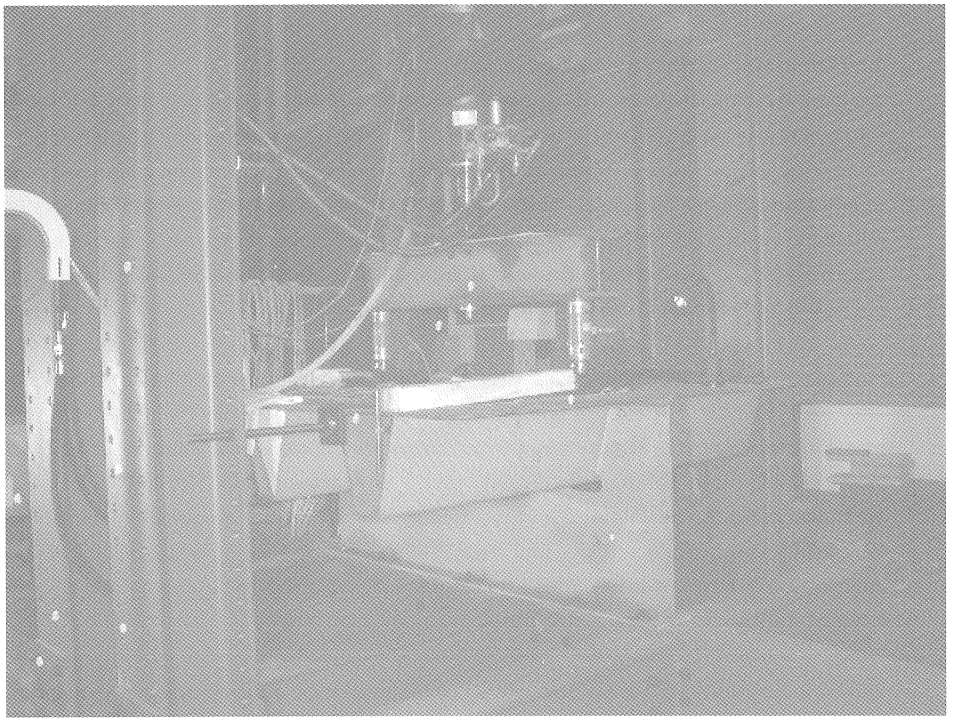

Figure 3: The fatigue set-up with loading at ribs 1 and 3.

pend the fatigue test, which happened each time the observed strain had risen more than 15% with respect to the previous inspection. After a suspension, the deck was first visually inspected for signs of cracks. Subsequently, the specimen was taken from the set-up and placed upside down to allow a more convenient ultrasonic data acquisition at the underside of the deck. After the ultrasonic measurements, the specimen is rebuild into the set-up to continue the cyclic loading.

In this fashion in total 8 inspections were carried out before the cracks came completely through the deck plate and had grown to a length of more than 125 mm. Inspection 0 is conducted before any loading was applied, and inspection 1 is conducted after a static pressure test to make sure that a static loading to a new specimen does not cause some detectable damage to the welds. The static test has been conducted only on the middle rib, so that inspection 1 yields data only for welds 'C' and 'D'. We note that, due to the stiffness of the ribs, the applied levels of loading may have a significant influence only on the welds nearest to the loading areas. Inspections 2 to 7 are conducted after the number of fatigue cycles as listed in Table 1 was reached.

3 Optimised ultrasonic measurement methods

3.1 Optimisation of the experimental set-up

The purpose of the ultrasonic set-up is to detect cracks, but the probability of detection with a given set-up depends sensitively on the type of crack. Therefore, if the number of measurements and/or types of transducers is not carefully chosen, there is a probability that certain cracks will go undetected. Moreover, even if a crack can be detected there is still a probability that its size cannot be determined with sufficient accuracy. Theoretically, to prevent both these problems one could take a huge number of measurements. This would assure that the inspection is reliable whatever the type of crack that is encountered in the bridge deck.

However, such an extended approach would not lead to a practicable inspection technique for a large steel structure. Therefore, it is highly desirable to reduce the number of required measurements to a minimum. To achieve this, first all the available apriori knowledge about the possible cracks has been used. For example, the most probable point of initiation (IP) and angle of the crack are shown in Fig. 2. The IP is introduced in support of a vast body of empirical evidence of where the cracks appear to initiate, which is at the root of the rib weld. The expectation value of the crack angle is 17 deg, but to overcome the possible spread the set-up has to be prepared for a possible range of crack angles between 0 deg and 35 deg.

Finally, wave path software has been employed to simulate the ultrasonic responses that can be expected for all the possible cracks. The wave path software calculated the possible wave paths in the plate when the transmitter and receiver types, their positions in a complete scan, and the location, depth and angle of the crack are input to the program. To stay on the safe side, the set-up is determined in such a way that every millimetre of the possible crack surface will be irradiated several times. The idea is that the more often the crack is detectably irradiated, the more reliable the inspection will be. This set-up optimisation is performed iteratively by trial and error and is used to determine the measurement techniques for both the crack depth and crack length detection as presented in this paper.

3.2 Crack depth detection method

In our specimen, a crack may start at the root of any of the six rib welds right above the girder. In these areas of the deck plate the main inspection interest is detection of the crack depth. It is common practice to determine the crack depth relative to the thickness d of the plate. Since the crack grows under an angle, it is understood that the crack depth is defined by the vertical distance between the lower deck plate surface - where it initiated- and the crack tip.

Since the physical presence of the girder obstructs positioning of transducers, a direct horizontally perpendicular irradiation of the crack is not possible. Therefore an angled pitch-catch technique [6] must be employed. This set-up is depicted in Fig. 4. The transmitter is positioned at one side of the girder and the receiver at the other side. Both probes are directed under a horizontal angle of 20 deg at the IP with the help of two Perspex triangles. The 20 deg angle is a compromise between try-

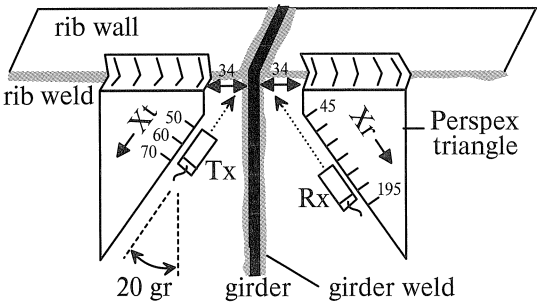

Figure 4: Pitch-catch set-up for crack depth detection. One of these inspection area is indicated by a circle in Fig. 1

ing to keep the angle as small as possible for optimum crack reflectivity, while at the same time minimizing the shortest possible distance between the wave probe and the crack. The triangles have millimetre indications at the sloping side to allow for a convenient and accurate probe positioning.

On a surface two positioning references are required to reproduce the measurement positions during different inspections. Note therefore that the ultrasonic measurements have to be repeated in different stages of the fatigue test. The first positioning reference is a fixed distance of 34 mm between the girder and the triangles. This distance is determined by the requirement that the transducers remain aimed at the IP. For the second reference the triangles rest against the sloping side of the rib. For this purpose one side of the triangle is adapted so it bridges the width of the rib weld. This was required since the weld is quite irregular, especially near the girder. The triangles can be clamped to the steel deck plate with a few magnets.

At each rib weld we took three sets of measurements along a straight line, (line scans). The three line scans are characterized by the horizontal distance between the transmitter and the IP. These distances are Xt=50 mm, Xt=60 mm and Xt=70 mm, where the origin Xt=0 lies in the IP. The wave paths from these transmitter positions towards the IP are depicted in a vertical cross section of the deck plate in Fig. 5. Note that this cross-section lies at a horizontal angle of 20 deg with respect to the girder. The wave paths show that the depth of the crack is completely irradiated by the three scans, especially since a probe in reality produces a beam of waves [6]. For each transmitter position, the receiver scans 31 positions in 5 mm steps from Xr=45 mm to Xr=195 mm, i.e. towards the IP in a straight line along the triangle, as shown in Fig. 4. The origin Xr=0 also lies in the IP.

The transmitter is a 70 deg shear wave probe and the receiver a 60 deg shear wave probe. The optimisation software showed that this probe combination performs best for the possible cracks in this inspection problem. Both transducers are equipped with a 3.5 MHz/0.5 inch piezoelectric transducer, which is a compromise between resolution and attenuation (both increase with frequency).

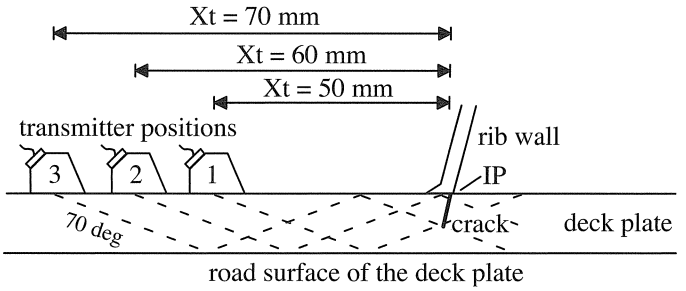

Figure 5: Vertical cross section of the pitch-catch set-up.

The vertical opening angles of the probes are determined at -26dB as 22 deg for the 70 deg probe and 28 deg for the 60 deg probe. The horizontal opening angle of the 70 deg probe is roughly 50% less than its vertical opening angle, which improves the selective horizontal irradiation of the location where the crack initiates.

At each receiver position 6001 time samples are acquired at 40 MHz sampling frequency (150 μs scan time) with a 12 bit amplitude quantization. The signal-to-noise ratio improved considerably by averaging 512 signals at each receiver position before storing the result on computer disk for signal analysis.

3.3 Crack length detection method

Once the crack has grown to a sufficient size it becomes detectable along the rib weld by using a horizontally perpendicular irradiation of the crack surface. In this stage, the crack length is of prime interest, rather than its maximum depth that is (supposedly) already known from the previous measurements. For this purpose the simpler pulse-echo [6] technique may be employed, which requires only one transducer. The horizontal orientation of the large crack may be no longer parallel to the rib weld, which is accounted for by allowing the probe to be swivelled up to ±10 deg to scan for the maximum response before storing the data. This set-up is depicted in Fig. 6.

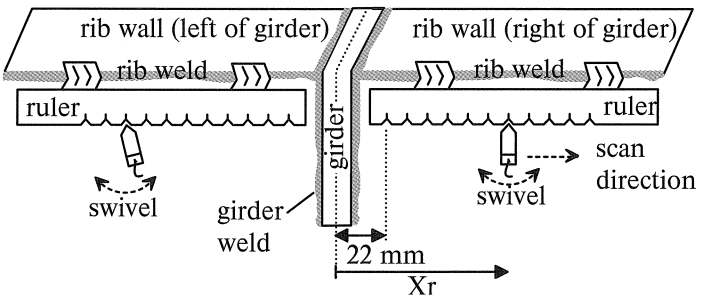

Figure 6: Pulse-echo set-up for crack length detection.

Two Perspex rulers have been designed and constructed to allow for a convenient and accurate probe positioning. Small indentations in the rulers create a swivel point without the chance of the probe slipping away from its current scan position. Note therefore that a gel couplant [6] is used for proper acoustical contact between a probe and the steel surface, which causes a slippery surface. The swivel feature is accommodated by the wedged-shaped front of the used type of probe. The rulers can be clamped to the steel deck plate with a few magnets.

On a surface two positioning references are required in order to reproduce the measurement positions during different inspections. Note therefore that the ultrasonic measurements are repeated in different stages of the fatigue test. The first positioning reference is a fixed distance of 22 mm between the middle of the girder plate and a ruler, which accounts for the thickness of the girder, the girder weld, and the probe itself. Therefore, the first accessible probe positions lie at Xr= ±22 mm, where the origin Xr=0 lies in the middle of the girder plate. For the second positioning reference the ruler rests against the sloping side of the rib. For this purpose the side of the ruler is adapted so it bridges the weld, as shown in Fig. 7.
To improve the detectability of the crack length two pulse-echo scans are taken. One scan is carried

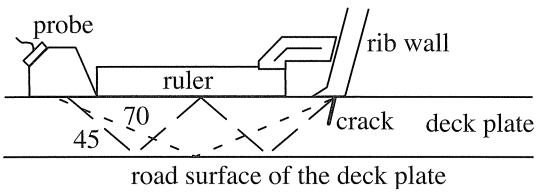

Figure 7: Vertical cross section of the pulse-echo set-up.

out with a 70 deg shear wave probe and the other with a 45 deg shear wave probe. Since the probes actually produce a beam of waves, these probes span a large range of vertical opening angles.
The width of the rulers is designed such that both probes give optimum irradiation of the rib weld, which is where the crack will appear first. The main irradiating wave paths are depicted in a vertical cross section of the deck plate in Fig. 7. We note that the centre of the smaller 45 deg probe lies 5 mm closer to the rib weld than the centre of the 70 deg probe.

Both transducers are equipped with a 3.5 MHz/0.5 inch piezoelectric transducer. Along each rib weld a line scan is taken in steps of 5 mm from Xr=-267 mm to Xr=-22 mm, and from Xr=22 mm to Xr=267 mm. The sampling and storage method is the same as described in Subsection 3.2.

4 Visual and ultrasonic inspection results

4.1 Visual inspection

It was not until inspection 6 that cracks became visible in the deck plate on the roadside, since they remain invisible from the underside of the bridge deck. The number of fatigue cycles when the first visual cracking occurred is added in row 'fvc' in Table 1. The crack lengths observed in inspection 7

are given in Table 2.

The shortest horizontal distance between the IP and the observed crack on the roadside of the deck plate gives information on the vertical crack angle. These measurements suggest that the crack angles are always steeper than 20 deg.

Table 1: Number of fatigue cycles before inspections 0 to 7.

inspection	ribs 1 and 3	rib 2
0	0	0
1	-	static
2	158333	186563
3	295409	229444
4	411378	312398
5	528020	480084
6	711788	733539
fvc	1140605	1561051
7	3056039	3205759

4.2 Peak amplitude as ultrasonic crack depth indicator

A commonly used crack indicator is the peak amplitude in the scanned data. The basic idea is that the detected peak amplitude proportionally increases with the reflective crack surface, i.e. crack size. The proportionality breaks down when the crack becomes larger than the area irradiated by the probes, or when the crack has completely broken through the deck pate. If $\hat{A}_{nm}$ indicates the absolute peak amplitude at the n^{th} receiver position in the m^{th} inspection, the crack indicator I_m^A is defined as the average over all 31 scan positions,

$$I_m^A = \frac{1}{31}\sum_{n=1}^{31} \hat{A}_{nm} \tag{1}$$

where m= 0,1,..7. The combination of three scans with three different transmitter positions ensures that the whole depth of the crack is irradiated, while taking the average improves the robustness of the method. The development of I_m^A through the subsequent inspections is plotted in Fig. 8 for rib welds 'A' to 'F'. The curves for the three different pitch-catch scans are indicated by the transmitter distances of 50, 60 and 70 mm.

From the trends in Fig. 8 we infer the first signs of fatigue damage already in inspection 2, except for welds 'C' and 'F' where it becomes detectable in inspection 3. The plots suggest that the cracks have developed quite differently. For weld 'B' the crack appears to be almost through the deck plate in inspection 3, since the level is similar to that in inspection 7. On the other hand, the crack in weld 'C' does not reach this stage until inspection 6.

The dips that occur in the same inspection in all three curves in Fig. 8, such as for weld 'C' in inspection 4, indicate a sudden reduction in the reflective surface of the crack. This uncontrollable

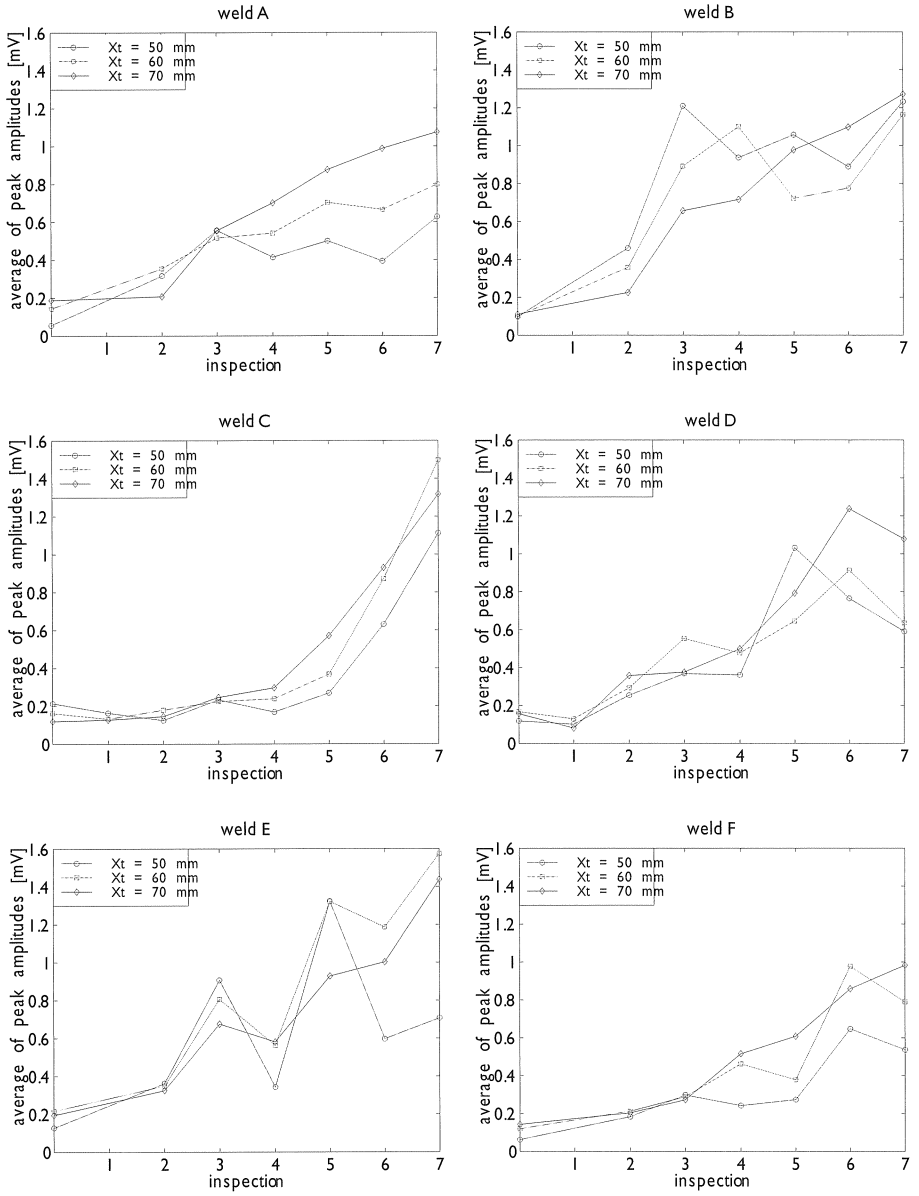

Figure 8: Average peak amplitude in the pitch-catch scans as a crack indicator.

effect is due to a partial contact between the opposite crack faces [11] that creates a partially ultrasonically transparent crack, which reduces the reflective crack surface. This crack closure is caused by stresses resulting from the proper weight (780 kg) of the bridge deck specimen and occurs when the bridge deck specimen is turned over to facilitate the underside ultrasonic measurements. It is expected that the chance of crack closure increase with increasing crack size, which explains why it becomes apparent only after inspection 3.

All three scans appear reliable for the purpose of crack detection, which indicates that the irradiation coverage of the crack is excellent at each transmitter distance. Nevertheless, since the crack is oriented at an angle, the most effective transmitter position will to some degree depend on the specific crack size and crack angle. This can be seen from the sensitivity for early fatigue damage, which appears best for Xt=50 mm where the transmitter is placed closest to the IP. On the other hand, the curves for Xt=70 mm show the most steady trend towards an average amplitude level of 1.2 mV in the final cracking stage of inspection 7. Therefore, the larger transmitter distance appears to be better suited for larger cracks.

To obtain a crack depth estimate we employ a robust calibration between peak amplitude and relative crack depth. The calibration is obtained by replacing the vertical scale in Fig. 8 by a linear scale indicating 0% to 100% crack depth, where 100% indicates complete cracking through the deck plate and complies with the value in inspection 7. Judging from the spread in the amplitudes in inspection 7, the accuracy of this estimate can be better than ±20%. Note that the reliability of this method is better for smaller cracks due to the reduced chance of crack closure.

4.3 Wave count as ultrasonic crack depth indicator

A very sensitive crack indicator is the number of detectable waves in the scanned data. The basic idea is that the number of waves proportionally increases with increasing crack size, since the crack reflects and scatters more waves, and also stronger waves. The proportionality breaks down when the crack becomes larger than the area irradiated by the probes, or when the crack has completely broken through the deck pate.

In this method, only the waves with amplitude higher than the detection level are counted. The detection level is determined from the amplitude levels for the uncracked stage (inspection 0) in Fig. 8 as 0.1 mV. This detection level prevents influences of all types of noise and gives an optimum sensitivity of the method for small cracks. A lower detection level would make the method more susceptible to noise and reduce the sensitivity for sizing of larger cracks. On the other hand, a higher detection level would make the method less sensitive to noise but also reduces the sensitivity for sizing of small cracks.

The detection level suppresses the waves that are scattered by the normal (undamaged) welds. We note that the unpredictable influence of a wear layer or coating in practical (in-situ) applications will also be reduced, since these affect mainly the amplitudes. If $\hat{W}_{mm}$ indicates the number of

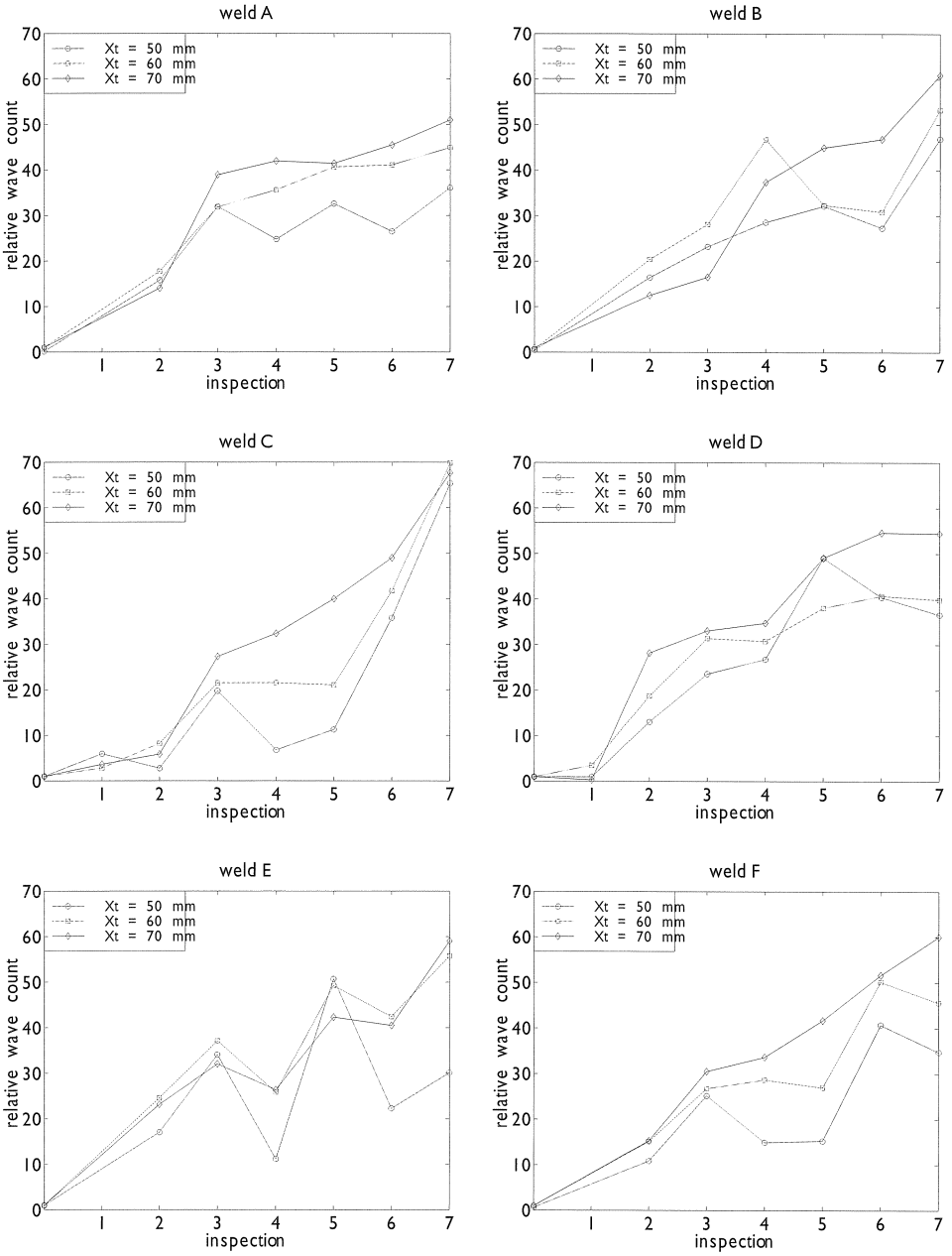

Figure 9: Average, normalized wave count in the pitch-catch scans as a crack indicator.

detected waves at the n^{th} receiver position in the m^{th} inspection, the crack indicator I_m^W is defined as the average over all 31 scan positions. Now, the exact number of wave counts in the uncracked state is actually irrelevant, and it may also vary to some degree from weld to weld. Therefore, all curves I_m^W for m=1,2,...7 are normalized to the wave count in inspection 0, after which we set $I_0^W = 1$. This leads to the definition

$$I_m^W = \frac{1}{I_0^W} \frac{1}{31} \sum_{n=1}^{31} \hat{w}_{nm} \tag{2}$$

where m=1,2,...7. The combination of three scans with three different transmitter positions ensures that the whole depth of the crack is irradiated, while taking the average improves the robustness of the method.

The development of I_m^W through the subsequent inspections is plotted in Fig. 9 for rib welds 'A' to 'F'. The curves for the three different pitch-catch scans are indicated by the transmitter distances of 50, 60 and 70 mm.

The curves indicate a much better sensitivity to early fatigue damage than the peak amplitude indicator. The wave count generally increases by a factor 10 to 30 from inspection 0 to inspection 2. Note that weld 'C', which shows no crack growth in Fig. 8, now shows an increase by a factor 8.

The plots show a similar trend: a rapid growth of the crack until inspection 3, and then a slower growth up to inspection 6 when they finally break through the deck plate. This trend points to a type of crack that first predominantly grows into the depth of the plate, and then at some point continuous with a predominantly horizontal growth (increasing crack length). At some point the increase in horizontal size is no longer detected, since the growth falls outside the ultrasonic irradiation of the transmitters. This is why the curves show a horizontal trend between inspections 3 to 6.

The curves for Xt=70 mm again show the most steady growth and in inspection 7 they reach an average level of 59, which corresponds to 100% cracking. To obtain a crack depth estimate we employ a simple calibration between the relative wave count and the relative crack depth. The calibration is obtained by replacing the vertical scale in Fig. 9 by a linear scale indicating 0% to 100% crack depth, where 100% indicates complete cracking through the deck plate and complies with the value in inspection 7. Judging from the spread in the wave counts in inspection 7, the accuracy of this estimate can be better than ±15%.

4.4 Peak amplitude as ultrasonic crack length indicator

The purpose of the pulse-echo scans along the rib welds is to detect the crack length. For this purpose the probe is not required to irradiate the whole depth of the crack, and the peak amplitude will be a sufficiently accurate crack length indicator. The peak amplitudes are plotted in Fig. 10 for the pulse-echo scan with the 70 deg probe, and in Fig. 11 for the pulse-echo scan with the 45 deg probe. Note that the plots start at the left side of the girder (negative Xr) and continue at the right side of the girder (positive Xr). The girder therefore obstructs measurements from Xr=-22 mm to Xr=22 mm.

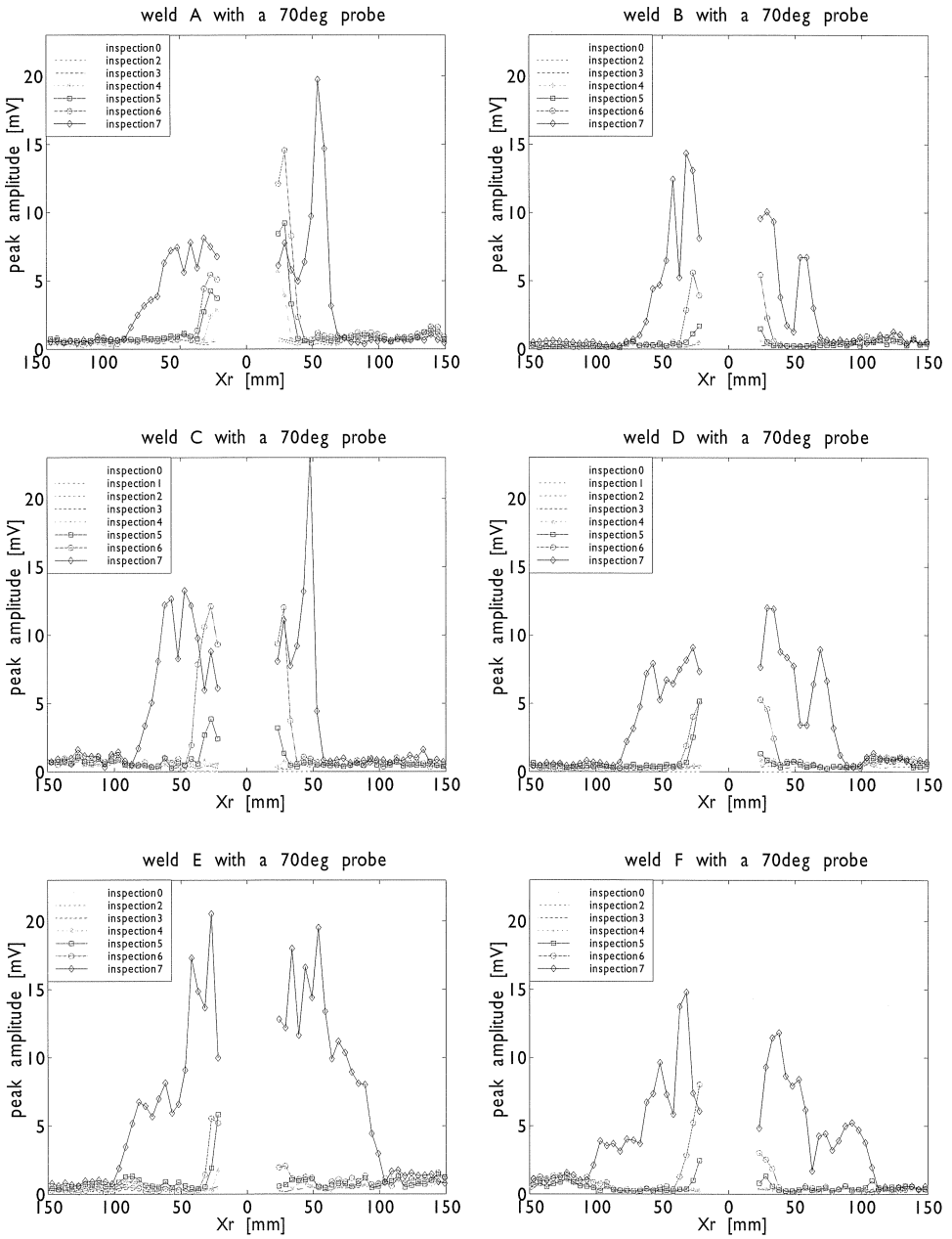

Figure 10: Peak amplitude in the 70 deg probe pulse-echo scans as a crack length indicator.

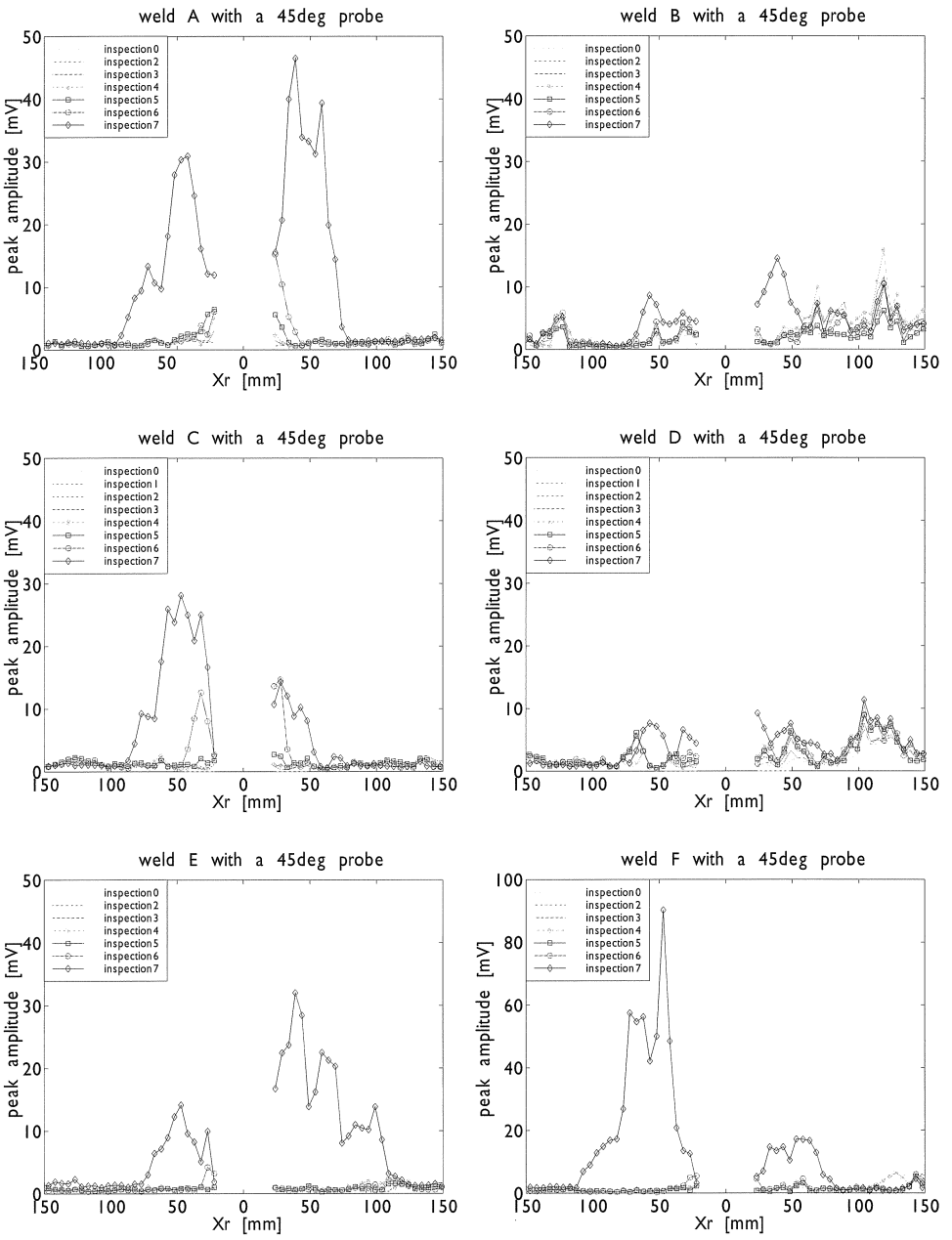

Figure 11: Peak amplitude in the 45 deg probe pulse-echo scans as a crack length indicator.

These measurements give new information on the crack development. Up to inspection 6 the cracks along the middle rib welds ('C' and 'D') developed relatively symmetrical with respect to the girder, in contrary to the cracks along the outer rib welds ('A', 'B', 'E' and 'F'). This is probably due to the two-axis loading, which leads more easily to asymmetrical loading when the cracks develop differently along the different rib welds and locally change the stiffness of the bridge deck.

The amplitudes for the 45 deg probe vary considerably. The cracks along 'B' and 'D' are hardly detectable, even in inspection 7 when the crack is completely through the deck plate. This indicates that these cracks have grown under a steeper angle, and present a larger reflective surface to the angled waves travelling under 70 deg.

Table 2: Ultrasonically determined crack lengths for inspections 4 to 7.

weld	insp. 4	insp. 5	insp. 6	insp.7	visual insp. (7)
A	72	74	86	171	165
B	-	70	76	161	136
C	-	70	84	145	150
D	-	79	91	181	155
E	-	52	71	206	201
F	-	70	85	220	208

For the 70 deg probe and inspections 4 to 7 the crack length is determined between the points where a curve is no longer distinguishable from the curves for inspections 0 to 3. The crack lengths are shown in Table 2. With the exception of rib weld 'C' the ultrasonic inspection gives evidence of a larger crack than visual inspection. This is expected, because the crack develops upward from the bottom of the deck plate.
Therefore, the length of the crack at the bottom of the deck plate is larger than the visible surface-breaking part at the road surface of the deck plate.

From the ultrasonic crack length data an estimate is obtained of the minimum ratio of absolute crack depth to absolute crack length, where the length is defined from crack tip to crack tip. Assuming that in inspection 6 the crack depth is 100% and thus 10.5 mm, then the crack lengths in Table 2 show that the ratio may vary from 1:7 to 1:9. These large ratios support our finding in Section 4.3 that in later stages of fatigue the cracks develop predominantly in a horizontal direction.

5 Conclusions

A new ultrasonic method is proposed that enables inspection of a steel orthotropic bridge deck from the underside of the deck plate. Specifically, the method enables detection of the crack that initiates where the deck plate, a rib and a girder are joined by a weld. These critical areas cannot be inspected by visual techniques.

The calibration between the ultrasonic crack indicators and the actual crack size is obtained by using ultrasonic data from a fatigue test on a representative bridge deck specimen. The test was regularly suspended, which allowed the acquisition of ultrasonic data of all stages of cracking.

The data shows that the probability of detection (POD) of the method is excellent. All the occurring cracks could be followed from initiation to the final stage of through-cracking. The method proves quite sensitive to small cracks, while the actual crack depth in the subsequent fatigue stages can be estimated with ±15% accuracy.

The method provides insight into the development of cracks, in particular for the type of crack mentioned above. This crack grows under a vertical angle that is steeper than 20 deg with respect to the vertical.
The ultrasonic results indicate two stages in its growth: first a predominant depth growth, which stops before through-cracking occurs, followed by a stage of predominant length growth. This finding is supported by the ultrasonic crack length measurements, which point to a long, shallow type of crack with a depth to length ratio between 1:7 and 1:9.

The ultrasonic method proves to be quite robust, which makes it suitable for in-situ bridge deck inspection, where the coating and the wear layer may cause additional amplitude variations and damping.

Acknowledgements

The research has been financially supported by the Dutch Technology Foundation (STW), which is gratefully acknowledged.

References

[1] A.R. Mangus, *Orthotropic design meets cold weather challenges: an overview of orthotropic steel deck bridges in cold regions*, Welding Innovation Vol.XIX no.1, (2002).

[2] C. Miki, M. Fukazawa, M. Katoh and H. Ohune, *Feasibility study on non-destructive methods for fatigue crack detection in steel bridge members.* Br.J.Non-Destr.Test. v.32 no.6, (June 1990), pp. 291-302.

[3] W.J. Zippel, J.A. Pincheira and G.A. Washer, *Crack measurement in steel plates using TOFD method*, J. of Perf. of Const. Fac. v.14 no.2, (2000), pp. 75-82.

[4] D.J. Yoon, J.C. Jung, P. Park and S.S. Lee, *AE characteristics for monitoring fatigue crack in steel bridge members*, Proc. of SPIE The Int. Soc. for Opt. Eng. v.3995 (2000), pp. 153-162.

[5] A. Ghorbanpoor and A.T. Rentmeester, *NDE of steel bridges by acoustic emission, Proc. Symp. Struct. Eng. Nat. Hazard Mitigation 1993*, ASCE New York (1993), pp. 1008-1013.

[6] J. Krautkamer and H. Krautkamer, Ultrasonic testing ofmaterials, (Springer-Verlag Berlin Heidelberg, 1990)

[7] M. Lorenz and T.S. Wielinga, *Ultrasonic characterization of defects in steel using multi-SAFT imaging and neural networks*, NDT&E-Int. 26(3), (June 1993), pp. 127-33.

[8] V. Schmitz, F. Walte and S.V. Chakhlov, *3D ray tracing in austenite materials*, NDT&E-Int. 32(4), (June 1999), pp. 201-13.

[9] A.A. Carvalho, L.V.S. Sagrilo, I.C. Silva and J.M.A. Rebello, *The POD curve for the detection of planar defects using a multi-channel ultrasonic system*, Insight NDT and Cond. Mon. v.44 no.11,(Nov. 2002), pp. 689-693.

[10] I.N. Komsky, *Application of portable modules for fatigue crack characterization*, Proc. of SPIE The Int. Soc. for Opt. Eng. v.4335 (2001), pp. 290-299.

[11] O. Buck, B.J. Skillings and L.K. Reed, *Simulation of closure: effects on crack detection probability and stress distributions*, Rev. Progr. QNDE 2A, (1983), pp. 345-52.